Progress In Electromagnetics Research M, Vol. 121, 1–11, 2023

Multi-Physics Analysis and Loss Evaluation of High Frequency Transformer with Non-sinusoidal Excitation

Sherin Joseph[1, 2, *], Shajimon K. John[3], Kudilil P. Pinkymol[4], Jineeth Joseph[5], and Kappamadathil R. M. Nair[6]

Abstract—High Frequency Transformer (HFT) acts as the key element of a Solid State Transformer (SST), which is a mandatory equipment in smartgrid system. SST replaces power frequency transformer by providing control and communication in power system. The design of an HFT matching the design of conventional distribution transformer is done in this paper. It is done by developing an iterative algorithm using Brute Force technique. The optimum design is selected by taking minimization of total owning cost as objective function. The algorithm takes eight design variables and four design constraints for shortlisting the optimum design. The optimum design developed is validated in finite element analysis software. The multi-physics analysis of the design is done by interconnecting electromagnetic, mechanical, thermal, and power electronics components of the system. The analytical and numerical analysis follow the same pattern by conducting a case study on the design of HFT with ratings 1000 kVA, 11 kV/415 V, three phases.

1. INTRODUCTION

Multi-physics analysis is a computational approach that combines multiple physical phenomena to study a complex system. This approach allows engineers to gain a deeper understanding of the system's performance to validate the design. This paper discusses the multi-physics analysis of a High Frequency Transformer (HFT) incorporated in distribution application Solid State Transformer (SST). Solid state transformer is emerging as the key element in smartgrid technology due to its multi-tasking capability compared with power frequency transformer. The key feature of SST in smartgrid environment are being able to precisely control and regulate voltage levels, easy integration of renewable energy sources, bidirectional and controlled power flow, enhanced grid stability during faults and fluctuations, power quality improvement, etc. The major components of SST are power electronics based converter/inverter circuits and high frequency transformer. The power electronic circuit includes AC to DC converter and DC to high frequency AC converter in high voltage (HV) side and high frequency AC to DC converter and DC to power frequency AC converter in low voltage (LV) side. The block schematic representation of SST is shown in Fig. 1.

The components and construction of HFT are similar to power frequency transformer. It consists of magnetic circuits known as core, electric circuit known as winding, dielectric circuit known as insulation, and other accessories such as tank, bushings, cooling system, and protective devices.

The design of SST for distribution application has been done by many researchers. The major research areas in SST are the development of medium voltage, high frequency power converters, and the development of high frequency transformer [1]. Different types of SST topologies are narrated in

Received 23 August 2023, Accepted 27 October 2023, Scheduled 8 November 2023

* Corresponding author: Sherin Joseph (sherinjoseph@ceconline.edu.com).
[1] Saintgits College of Engineering, Kerala, India. [2] APJ Abdul Kalam Technological University, Kerala, India. [3] Muthoot Institute of Technology and Science, Ernakulam, Kerala, India. [4] National Institute of Technology Thiruchirappalli, India. [5] GKN Fokker Elmo BV, Netherlands. [6] Transformer Design and Testing, Kottayam, Kerala, India.

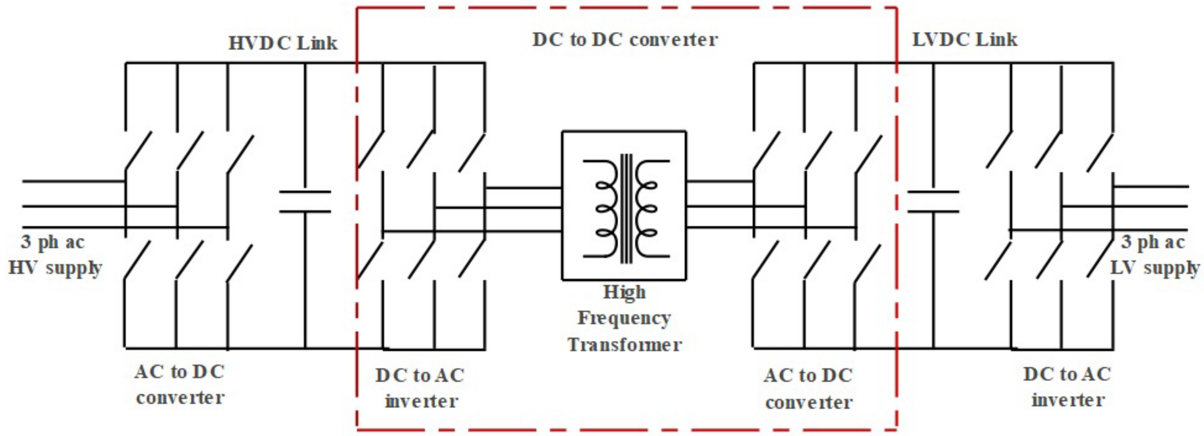

Figure 1. Structure of SST.

literature based on the power converter stages and configuration, among which three stage SST topology shown in Fig. 1 is most common [2]. The key features of three stage SST topology are availability of low voltage DC link to feed DC loads and to connect renewable energy sources. Unidirectional or bidirectional power flow of real and reactive power, power flow control, and power factor improvement are also possible in three stage SST topology [3]. The high voltage AC-DC converter in three stage topology is mainly multilevel type to withstand high voltage switching conditions [4]. In [5], SiC based MOSFETs/IGBTs are used for manufacturing multilevel converters. The high cost of these switches is the major limitation in the development of SST. Handling high voltage is the major challenge in the design of converters used in HV side, and high current capacity requirement is the major challenge in the design of converters used in LV side. In order to meet the above requirements, series connection is done in HV side converters, and paralleling is done in LV side [6]. The methods used for the design of high frequency transformer is narrated in [7–12]. The major design objectives of HFT discussed in these papers are reduced size, weight, cost, volume, etc.

In [7], the design and development of HFT for SST application is discussed, in which HFT is designed to maximize the transformer efficiency. The study performed in [8] introduces an optimization technique to find the frequency of operation of HFT at reduced volume. A 10 kVA prototype development is done in [9], where magnetic optimization is done to maximize the efficiency of transformer. Banumathy and Veeraraghavalu [10] discuss a new design procedure for the design of HFT by optimizing core geometry, which has a direct effect on regulation and copper losses. The design and development of a 100 kW, 1.2 kV, 20 kHz, 3 phase medium frequency transformer are explained in [11]. Here the design is done to check the feasibility of high power medium frequency 3 phase SST. Multi-physics based multi-objective optimization of 20 kW, 10 kHz HFT is investigated in [12]. Here core dimensions and optimal number of turns are taken as design variables, and the selection of only off the shelf core dimension is done after optimization. This paper considers two variables and one constraint for the optimum design of HFT for SST application. None of the above designs considered a power and voltage rating matching the conventional distribution transformer. High voltage rating was achieved only through cascading of a number of modules, which increases the overall size and complexity. Cost optimization is a critical requirement for the design and development of any product intended for commercial use. Since the aim of developing SST is to replace conventional power frequency transformer in distribution application, the cost analysis of SST must match the conventional transformer cost analysis. In conventional transformer the cost is calculated by considering the cost of losses along with the capital cost. The term used to describe loss capitalization along with product cost is called Total Owning Cost (TOC) of transformer [13]. For the development of an optimum design, an SST design that meets the above HFT design constraints must be considered. The costs of power electronic circuits for a specific power and voltage rating are the same. In order to calculate the TOC of SST, it is only significant to calculate the TOC of high frequency transformer [14].

In this paper, the authors would like to discuss the analysis, design, and validation of a high frequency transformer for incorporating with a distribution application SST. The objective function considered in this design is the minimization of TOC. An iterative algorithm using Brute force technique is developed for the optimum design. Eight design variables and four design constraints are taken while developing the iterative algorithm. Multi-physics analysis of one design selected from the iterative algorithm is done in ANSYS software, and the losses, flux and current distribution, and temperature rise are calculated. The paper is concluded with the comparison of the results obtained in analytical and finite element methods (FEMs).

2. BRUTE FORCE ALGORITHM FOR HFT DESIGN

Brute Force algorithm is a direct approach to solve a problem by exhaustively trying all possible solutions [15]. All possible combinations of results are systematically checked in this algorithm and generate optimum design based on the objective function given. This algorithm is adopted in this paper for the design of high frequency transformer for SST application.

The specifications required for calculating the optimum design of HFT are similar to the specification given for manufacturing a conventional distribution transformer. The authors in this paper are demonstrating the design of HFT incorporated in a 1000 kVA 11 kV/415 V, 3-phase SST. The power electronics part of this SST is another broad area of research and is not considered in this work. The voltage obtained at the HV side of the HFT is 10500 V for 11000 V applied at the input of SST [16]. Similarly, the output voltage of HFT must be 436 V to get 415 V at SST terminal. The variables considered for iteration in this work are the frequency, transformer constant k, width of core lamination, flux density of magnetic material, and conductor dimensions of HV and LV. The total owning cost and cost due to losses are calculated based on [17]. TOC can be expressed as

$$TOC = Initial\ Cost\ of\ Transformer\ in\ \$ + A \times No\ Load\ Losses + B \times Load\ Losses \tag{1}$$

where A is the cost of no load losses in $\$/W$ and is calculated using Equation (2).

$$A = \frac{8.76 \times P \times [1 - 1/(1+r)^n]}{r} \tag{2}$$

where P is the cost of one unit of energy in \$, r the discounting rate in p.um and n the transformer life time in years. The coefficient B, the cost of load losses in $\$/W$, can be obtained from (3)

$$B = L.F^2 \times A \tag{3}$$

where $L.F$ is the load factor. Load loss is proportional to the square of the transformer loading, which is again proportional to the square of the load factor. Provision is given in the algorithm for entering these parameters. The cost of raw materials at the time of design is entered in the algorithm. The optimum design developed from iterative algorithm must satisfy certain constraints for its practical implementation. The constraints considered in this design are flux density, percentage impedance, winding temperature rise, and fault current temperature rise. The limiting value of this constrains depends on the magnetic material, conductor, insulation material, etc.

The details of iterating parameters, specifications of HFT, design constraints, cost of raw material, capitalization cost details, etc. entered for obtaining optimum design from iterative algorithm are given in Tables 1, 2, and 3, respectively.

The options for selecting one core material from amorphous 2605SA1, nanocrystalline FT-3L and si-steel JNEX900 and options for selecting AC test voltage from 28 kV, 38 kV, 50 kV, and 70 kV are the special features of this algorithm. The steps involved in the algorithm are detailed below:

Step 1: Enter the details given in Tables 1, 2, and 3 and take the initial values of all design variables.

Step 2: Calculate per phase HV and LV.

Step 3: Calculate HV and LV line current.

Step 4: Calculate volt per turn ($Volt/turn = k \times \sqrt{Q}$).

Step 5: Calculate the number of turns in LV and round up to next integer and recalculate volt per turn.

Table 1. Details of the iterating parameters.

Design Variables	Min. Values	Step size	Max. Values	Count
Frequency (H_z)	200	200	5000	24
Flux density (T)	0.2	0.05	1.45	25
k value	0.8	0.8	4	4
HV width (mm)	4.5	0.8	8.5	5
HV thickness (mm)	0.8	0.24	2.5	7
LV sheet width (mm)	300	50	550	5
LV sheet thickness (mm)	0.7	0.3	2	5

Table 2. Specification and constraints of the optimum design.

Machine Details	Cut-off values
Rating of Transformer — 1000 kVA	B_m — 1.5 T
LV/ HV Voltage — 415/11000 V	$\%Z$ — 15%
Type of Insulation — Class F	Max. Temp. at short circuit — 350°C

Table 3. Rate of material and capitalization details.

Rate of Material	Capitalization
Amorphous — 3.5 $/kg	Energy Cost — 0.07 $/kWhr
Rate of Insulation — 7.84 $/kg	Discount Rate — 12%
Rate of Copper — 10 $/kg	Life Cycle — 25 yrs
Price of Fan — 160 $	Load Factor — 0.4

Step 6: Calculate HV number of turns and round up to the next integer.

Step 7: Calculate ratio error ($\frac{Nominal\ turns\ ratio - Actual\ turns\ ratio}{Nominal\ turns\ ratio} \times 100$).

Step 8: Calculate core dimensions (Net iron area from emf equation and gross iron area considering stacking factor [14]).

Step 9: Width and thickness of core lamination of wound core structure are calculated by taking the industry practice, i.e., $thickness = (1/3\ to\ 1/2\ of\ width\ of\ lamination)$.

Step 10: Recalculate the gross iron and net iron area based on thickness width values calculated from Step 9 and recalculate flux density based on new net iron area. Check whether the calculated B_m is within the limit else increment to the next iteration (Step 4).

Step 11: Calculate the area of cross section of LV winding foil type conductor using width and thickness from the range of LV dimensions given in Table 1.

Step 12: Calculate the current density and check whether it is within the limit for a particular foil type material else increment to the next iteration (Step 4).

Step 13: Calculate wound height, window height, and thickness of LV winding.

Step 14: Calculate area of cross section of HV winding from the dimensions given in Table 1. Step 12 should be followed for HV windings as well.

Step 15: Knowing the wound height from Step 13 and conductor dimension including insulation, the turns per layer and number of layers of HV winding can be calculated.

Step 16: Percentage reactance can be calculated using the equation given in [17]. Calculate $\%Z$ and check whether this value is within the limit given in Table 2.

Step 17: Load loss calculation of individual windings, considering skin and proximity effect due to high frequency application, is done based on [15].

Step 18: Volume of insulation is calculated by knowing the total volume of transformer and volume of core and winding. The weight of insulation is calculated from volume and density.

Step 19: Core loss calculation is done by calculating the weight of core and knowing the specific core loss from magnetic material data sheet.

Step 20: Short circuit withstanding capacity of individual winding is calculated [17], and check whether the design is within the limit.

Step 21: Cooling system design is done, by selecting fan and/or duct or natural cooling for keeping the winding temperature with in the limit specified in IEC standard [18].

Step 22: The design which satisfies all four constraints can go for calculating TOC. Calculate TOC of all healthy designs.

Step 23: Shortlist the optimum design with minimum TOC from the designs obtained in Step 22.

The dimensional, electrical, mechanical, and thermal parameters of HFT incorporated in 1000 kVA, 11 kV/415 V, 3 phase, Dyn11 SST, is obtained after iterating the above algorithm by giving input parameters given in Tables 1, 2, and 3. These parameters are listed in Table 4.

Table 4. Optimum design data of HFT.

No load Voltage (HV)	10500 V
No load Voltage (LV)	435 V
Optimum Frequency of Operation	600 Hz
Rated Current on HV	54.98 A
Rated Current on LV	1327.96 A
Current density (LV winding)	3.4 A/mm^2
Current density (HV winding)	4.14 A/mm^2
Conductor Dimension, HV	1.04×7.7 (mm)
Conductor Dimension, LV	1.3×300 (mm)
Flux Density	0.943 T
Number of Turns in HV	210
Number of Turns in LV	5
Core Width	170 mm
% Impedance (Z)	3.27%
No Load Losses	1141 W
Load Losses	2683 W
Max. Winding Temperature Rise	100°C
Insulation Class	Class F
Type of Cooling	AN-AF (one fan and one duct)
Fault Current in Temperature Rise	332°C
Weight of the Transformer	510 kg
Capital Cost	2600 $
Total Owning Cost	12000 $

The optimum design is developed by considering 21,00,000 design data inputs. The one design which has minimum TOC is listed in Table 4. This algorithm can also be utilized for developing the design with another power or voltage rating by entering the required parameter as input. It is possible

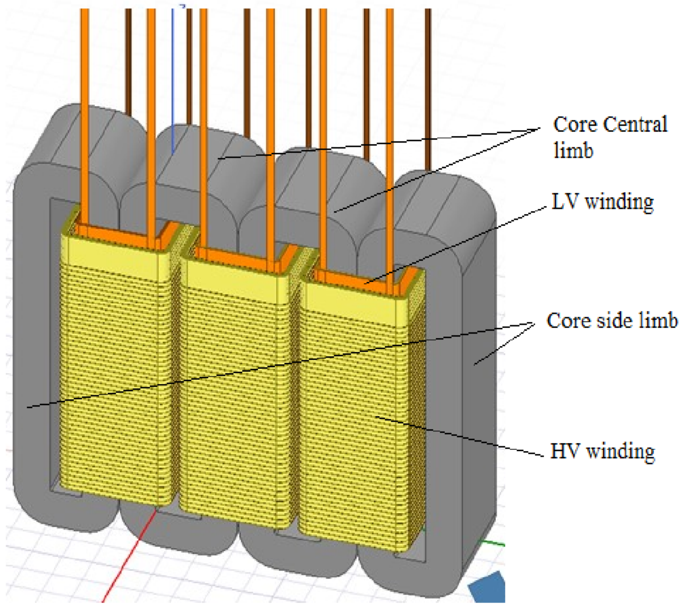

Figure 2. Structure of HFT optimum design.

to change the objective function as design with minimum capital cost or weight by changing the last step of algorithm after short listing the healthy designs. The three dimensional view of transformer after assembling is shown in Fig. 2.

3. MULTI-PHYSICS ANALYSIS OF THE OPTIMUM DESIGN

Multi-physics analysis refers to the study and simulation of physical properties related to different disciplines of physics such as mechanics, electromagnetics, and heat transfer. The behavior of the system is studied by considering the interactions and inter dependencies between various physical processes. The major steps involved in multi-physics analysis are problem definition, mathematical modeling, coupling and simulation, validation, analysis and interpretation. There are different softwares available for performing the multi-physics analysis, and ANSYS software is used in this work. Co-simulation of ANSYS Maxwell, ANSYS Mechanical and ANSYS Simplorer is done here. The problem definition in this analysis is the co-simulation of electromagnetic, mechanical, thermal and power electronics part of the developed high frequency transformer. Physical model of the HFT is developed in electromagnetic platform. Coupling is done through ANSYS mechanical to transient thermal for performing temperature rise test. Non-sinusoidal input to the HFT transformer is given from ANSYS Simplorer as shown in Fig. 3.

The input is given through a pulse width modulation (PWM) controlled two level inverter. The input voltage given and current taken to the HFT from DC-AC inverter are shown in Fig. 4.

The output voltage and current signal obtained from high frequency transformer is shown in Fig. 5.

The core loss plot of the HFT model is obtained by adding the properties of Amorphous (2605SA1) core material, into the 'add core material' option given in the 3D model development window of ANSYS Maxwell. The specific core loss and BH curve details of amorphous core material are taken from its data sheet. This data is used for constructing the core material in Maxwell platform. The output obtained for a 3 msec iteration is shown in Fig. 6. The load loss plot is obtained by considering all winding in HV and LV sides. The high frequency effect can be incorporated in the analysis by taking 'stranded loss AC' as output. The load loss plot is also shown in Fig. 6. Load loss and core loss characteristics show a steady response and near the calculated values. The behavior of HFT model to non-sinusoidal input also matches the analytical results.

The flux density and current density distribution of the HFT model is shown in Fig. 7. The

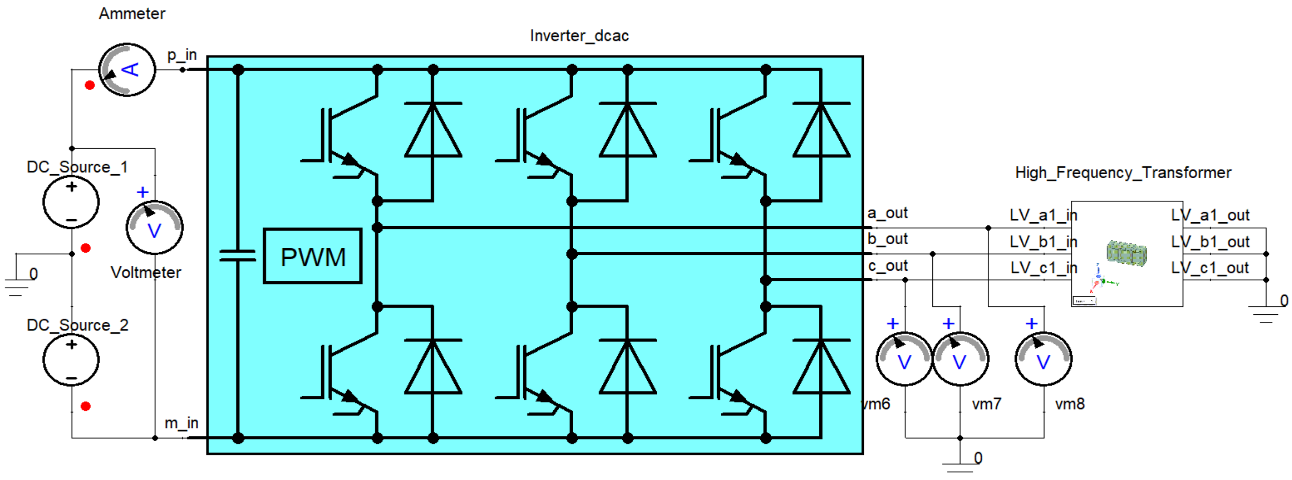

Figure 3. Connection diagram of HFT for non-sinusoidal excitation.

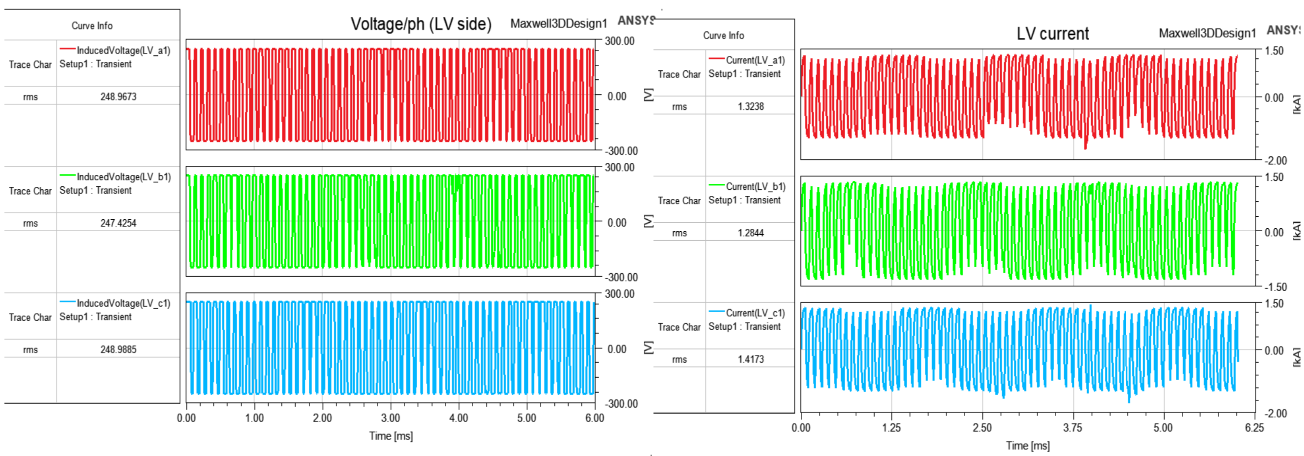

Figure 4. Input signal given to HFT from two-level inverter.

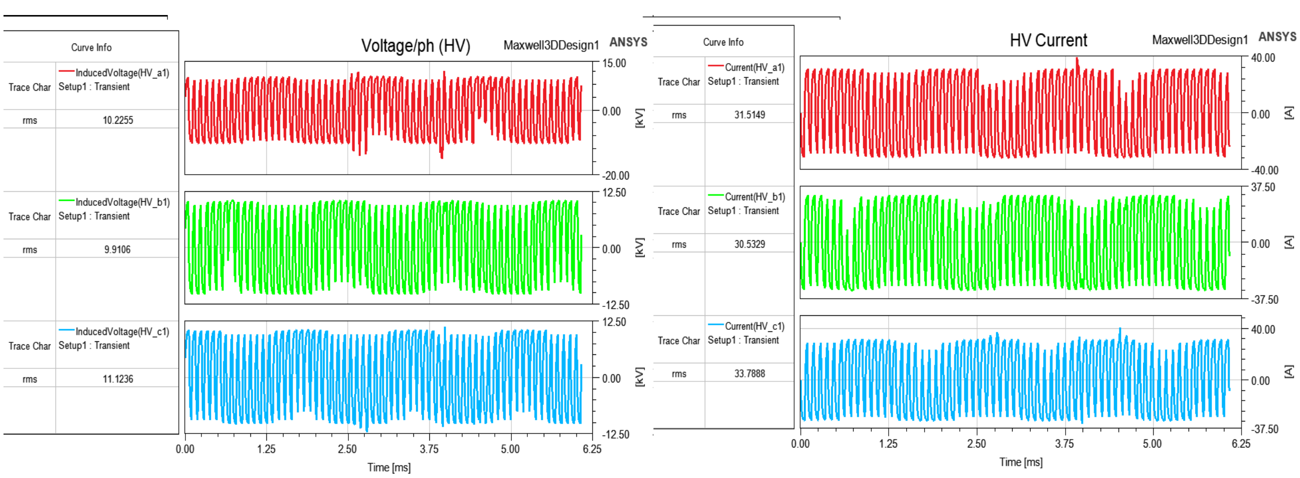

Figure 5. HFT output voltage and current.

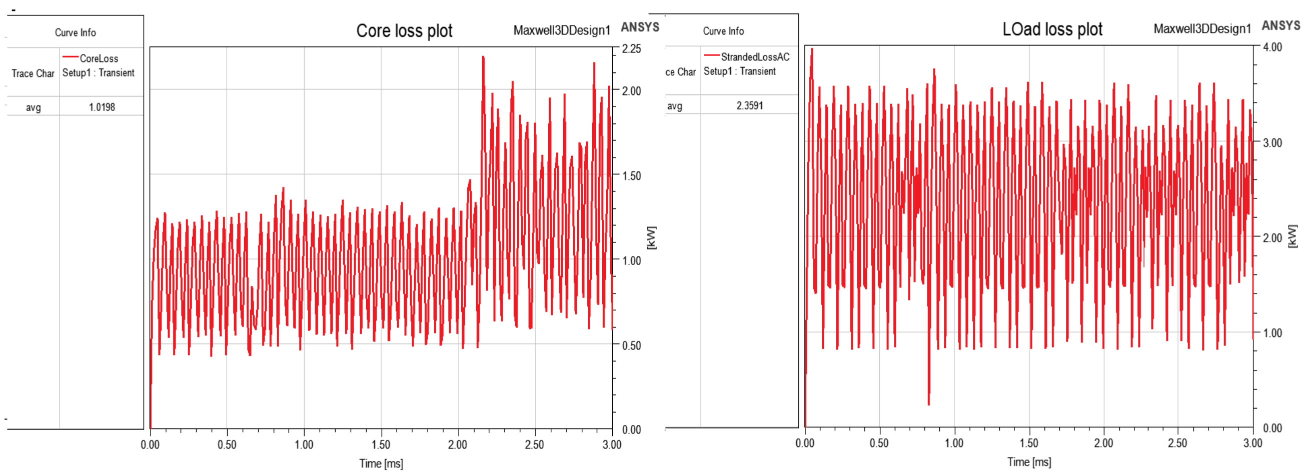

Figure 6. Core loss and load loss plot.

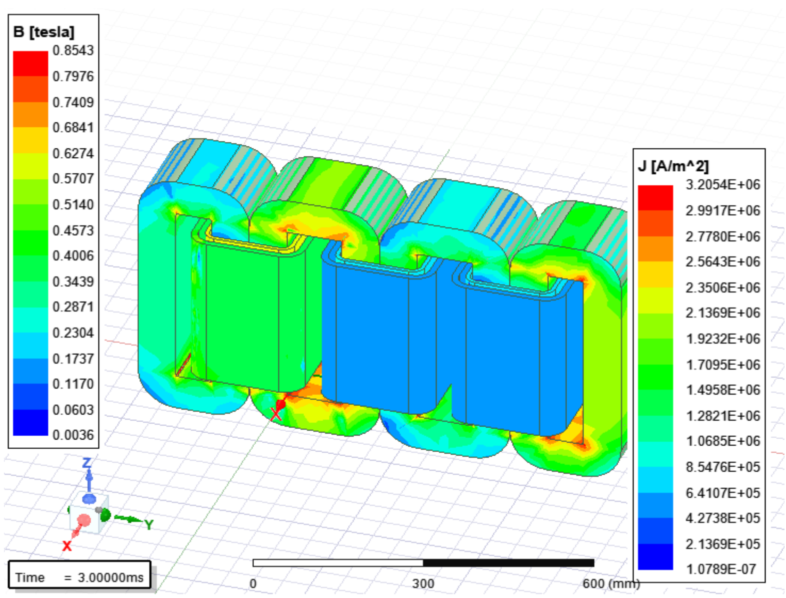

Figure 7. Flux density and current density distribution.

maximum flux density is less than 0.8543 T, and current density is less than 3.2 A/mm^2.

The multi-physics analysis of the optimum design developed in ANSYS Maxwell is done by interconnecting the model with ANSYS Mechanical through workbench. Transient thermal analysis is done in mechanical platform for performing temperature rise test. The temperature distribution obtained is less than 100°C. The temperature rise at different parts of HFT is shown in Fig. 8.

4. RESULTS AND DISCUSSION

The optimum design of the high frequency transformer with minimum total owning cost as objective function is designed and validated. The analytical design is performed using iterative algorithm. Brute Force technique is adopted for developing iterative algorithm. The optimum design is selected by considering 21,00,000 design data, and 2,58,272 healthy designs are short listed from that after satisfying four constraints. The optimum design is selected from these healthy designs after evaluating TOC. The optimum design with minimum TOC is modeled in finite element analysis software. Multi-

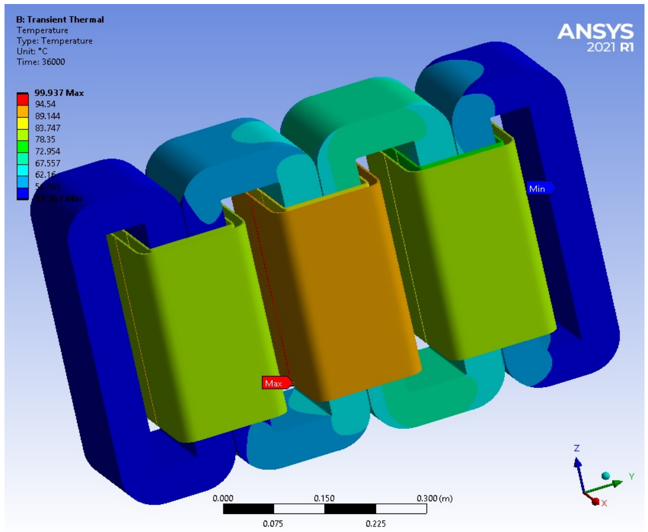

Figure 8. Temperature rise at different parts of HFT.

physics analysis of the optimum design is performed by interconnecting the electromagnetic, mechanical, thermal and power electronics parts. The results obtained match the analytical values. The parameters calculated in analytical and numerical methods are detailed in Table 5.

Table 5. Analytical vs. numerical results.

Parameters	**Analytical method**	**FEA method**
No load losses	1141 W	1019.8 W
Load losses	2683 W	2359 W
Flux density	0.943 T	0.8543 T
Current density	$3.4\,\mathrm{A/mm^2}$	$3.2\,\mathrm{A/mm^2}$
Temperature rise	$< 100°\mathrm{C}$	$< 100°\mathrm{C}$

The results of power power frequency transformer design considered in [14] give a load loss of 9000 W and no load loss of 1550 W for the same 1000 kVA rating. Moving from power frequency transformer to high frequency transformer, the overall dimension, losses, and TOC are considerably reduced. However, the cost of power electronic parts connected at both sides of HFT shown in Fig. 1 is very high. While moving from conventional grid to smartgrid, power electronic controllers are mandatory requirements in all power system elements such as in generation, transmission, and distribution side. The generalization of high voltage power switches reduces its manufacturing cost and cheaply available in the near future. The papers discussed in the literature do not consider the TOC as objective function, so the results obtained are not able to compare with the literature data.

5. CONCLUSION

The analytical design of high frequency transformer is done to develop optimum design by iterating a generalized algorithm. Eight design variables are iterated, and healthy designs are shortlisted by considering four design constraints. The optimum design with minimum TOC is shortlisted for validation. The validation is done by performing finite element analysis in ANSYS software. The results obtained are in close circle, and this iterative algorithm can enhance the development of HFT for SST application.

ACKNOWLEDGMENT

The authors would like to thank Centre for Engineering Research and Development (CERD), APJ Abdul Kalam Technological University Kerala, India for selecting this work for research seed money funding (KTU-RESEARCH-2/4643/2020).

REFERENCES

1. Kolar, J. W. and G. Ortiz, "Solid-state-transformers: Key components of future traction and smart grid systems," *Proc. IEEE Intern. Power Electronics Conf.*, Hiroshima, Japan, 2014.
2. She, X., R. Burgos, G. Wang, F. Wang, and A. Q. Huang, "Review of solid state transformer in the distribution system: From components to field application," *2012 IEEE Energy Conversion Congress and Exposition (ECCE)*, 4077–4084, Raleigh, NC, USA, 2012, doi: 10.1109/ECCE.2012.6342269.
3. Rehman, A. and M. Ashraf, "Design and analysis of PWM inverter for 100 kVA solid state transformer in a distribution system," *IEEE Access*, Vol. 7, 140152–140168, 2019, doi: 10.1109/ACCESS.2019.2942422.
4. Chaturvedi, P. K., S. K. Jain, P. Agrawal, and P. K. Modi, "Investigations on different multilevel inverter control techniques by simulation," *2006 International Conference on Power Electronic, Drives and Energy Systems*, 1–6, New Delhi, India, 2006, doi: 10.1109/PEDES.2006.344425.
5. Madhusoodhanan, S., A. Tripathi, D. Patel, K. Mainali, et al., "Solid-state transformer and MV grid tie applications enabled by 15 kV SiC IGBTs and 10 kV SiC MOSFETs based multilevel converters," *IEEE Transactions on Industry Applications*, Vol. 51, No. 4, 3343–3360, Jul.–Aug. 2015, doi: 10.1109/TIA.2015.2412096.
6. Wang, D., J. Tian, C. Mao, et al., "A 10-kV/400-V 500-kVA electronic power transformer," *IEEE Transactions on Industrial Electronics*, Vol. 63, No. 11, 6653–6663, Nov. 2016, doi: 10.1109/TIE.2016.2586440.
7. Montoya, R. J. G., "High-frequency transformer design for solid-state transformers in electric power distribution systems," University of Arkansas, 2015.
8. Bahmani, M. A., T. Thiringer, A. Rabiei, and T. Abdulahovic, "Comparative study of a multi-MW high-power density DC transformer with an optimized high-frequency magnetics in all-DC offshore wind farm," *IEEE Transactions on Power Delivery*, Vol. 31, No. 2, 857–866, Apr. 2016, doi: 10.1109/TPWRD.2015.2494883.
9. Lee, Y., G. Vakil, A. J. Watson, and P. Wheeler, "Geometry optimization and characterization of three-phase medium frequency transformer for 10 kVA isolated DC-DC converter," *2017 IEEE Energy Conversion Congress and Exposition (ECCE)*, 511–518, 2017, https://doi.org/10.1109/ECCE.2017.8095826.
10. Banumathy, J. R. and R. Veeraraghavalu, "High frequency transformer design and optimization using bio-inspired algorithms," *Applied Artificial Intelligence*, Vol. 32, Nos. 7–8, 707–726, 2018, doi: 10.1080/08839514.2018.1506969.
11. Dworakowski, P., A. Wilk, M. Michna, B. Lefebvre, and T. Lagier, "3-phase medium frequency transformer for a 100 kW 1.2 kV 20 kHz dual active bridge converter," *IECON 2019 — 45th Annual Conference of the IEEE Industrial Electronics Society*, 4071–4076, Lisbon, Portugal, 2019, doi: 10.1109/IECON.2019.8926695.
12. Olowu, T. O., H. Jafari, M. Moghaddami, and A. I. Sarwat, "Multiphysics and multiobjective design optimization of high-frequency transformers for solid-state transformer applications," *IEEE Transactions on Industry Applications*, Vol. 57, No. 1, 1014–1023, Jan.–Feb. 2021, doi: 10.1109/TIA.2020.3035129.
13. Thango, B. A., J. A. Jordaan, and A. F. nnachi, "Total ownership cost evaluation for transformers within solar power plants," *2020 6th IEEE International Energy Conference (ENERGYCon)*, 302–307, Gammarth, Tunisia, 2020, doi: 10.1109/ENERGYCon48941.2020.9236613.

14. Joseph, S., S. K. John, K. P. Pinkymol, J. Joseph, and K. R. M. Nair, "Multiphysics analysis of high frequency transformers used in SST with different magnetic materials," *Progress In Electromagnetics Research M*, Vol. 116, 129–143, 2023.
15. Mogorovic, M. and D. Dujic, "Medium frequency transformer leakage inductance modeling and experimental verification," *2017 IEEE Energy Conversion Congress and Exposition (ECCE)*, 419–424, Cincinnati, OH, USA, 2017, doi: 10.1109/ECCE.2017.8095813.
16. Joseph, S., A. K. Abraham, P. Harikrishna Raj, J. Joseph, and K. R. M. Nair, "An iterative algorithm for optimum design of high frequency transformer in SST application," *IECON 2020 The 46th Annual Conference of the IEEE Industrial Electronics Society*, 1538–1543, Singapore, 2020, doi: 10.1109/IECON43393.2020.9254914.
17. Nair, K. R. M., *Power and Distribution Transformers: Practical Design Guide*, 1st Edition, CRC Press, 2021, https://doi.org/10.1201/9781003088578.
18. IEC 60076-11: Power transformers — Part 11: Dry type Transformers, 2018.